

## CONSTRUCTION OF A HIGH-RESOLUTION 3-DIMENSIONAL S-WAVE VELOCITY STRUCTURE MODEL BASED ON JOINT INVERSION METHOD INTEGRATING VARIOUS KINDS OF GEOLOGICAL AND GEOPHYSICAL DATA

G. KOBAYASHI<sup>1</sup> and Y. MAMADA<sup>1</sup>

<sup>1</sup> Regulatory Standard and Research Department Secretariat of Nuclear Regulation Authority (S/NRA/R), Tokyo, Japan

*E-mail contact of main author: genyu\_kobayashi@nsr.go.jp*

**Abstract.** On 16th of July, 2007, the 6.8 magnitude Niigata-ken Chuetsu-oki Earthquake occurred near the Kashiwazaki-Kariwa NPP site. The maximum acceleration observed on the base mat of the 4 units located at the southwest side was almost two times greater than that of the 3 units located at the northeast side. It was revealed that spatial variation of the ground motions was caused by such factors as the complexity of the subsurface structure extending from the seismic bedrock ( $V_s=3\text{km/s}$ ) at a depth of 5 to 7 km to the building foundation ground. To explore more sophisticated ways to evaluate deep subsurface structure, we conducted a 3,000 m deep boring that reaches bedrock equivalent to seismic bedrock as well as a vertical seismic array observation at five depths of 0, 100, 550, 1,500 and 3,000 m in a deep borehole beneath the Niigata Institute of Technology campus located 10 km south of the Kashiwazaki-Kariwa NPP. In addition, we conducted a horizontal seismic dense array observation composed of 28 stations with spacing of about 7 m to 6 km, and a comprehensive deep subsurface structure survey through various geophysical explorations in and around the campus. To increase the accuracy of strong motion evaluation, we constructed high-resolution 3-dimensional S-wave velocity structure models for ground motion evaluation based on a joint inversion method integrating various kinds of geological and geophysical data, and carried out seismic wave propagation simulation. As a result, we can see that the accuracy of seismic wave propagation simulation of short period ground motions of 0.5-0.2 s can be improved by using a high-resolution model.

**Key Words:** Ground motion, Subsurface structure, Joint inversion, S-wave velocity structure model

### 1. INTRODUCTION

On 16th of July, 2007, the 6.8 magnitude Niigata-ken Chuetsu-oki Earthquake occurred near the Kashiwazaki-Kariwa NPP site. The ground motions observed at the site far exceeded the design ground motion assumed under the former Regulatory Guide for Seismic Design of Nuclear Power Plants (NSC Regulatory Guide (L-DS-1.0) in 1981). The maximum acceleration observed on the base mat of the 4 units located at the southwest side was almost two times greater than that of the 3 units located at the northeast side.

It was revealed that this spatial variation of the ground motions was caused by such factors as the complexity of the subsurface structure extending from the seismic bedrock ( $V_s=3\text{km/s}$ ) at a depth of 5 to 7 km to the building foundation ground (JNES, 2013 [1]). We learned a valuable lesson that more sophisticated methods for assessing the subsurface structure are essential in order to secure the seismic safety of nuclear facilities.

To explore sophisticated ways to evaluate deep subsurface structure, we conducted a 3,000 m deep boring that reaches bedrock equivalent to seismic bedrock as well as a vertical seismic array observation at five depths of 0, 100, 550, 1,500 and 3,000 m in a deep borehole beneath the Niigata Institute of Technology campus located 10 km south of the Kashiwazaki-Kariwa NPP. In addition, we conducted a horizontal seismic dense array observation composed of 28 stations (JNNK1-JNNK28) with spacing of about 7 m to 6 km, and a comprehensive deep subsurface structure survey through various geophysical explorations in and around the campus. To increase the accuracy of strong motion evaluation using seismic wave propagation simulation, we built high-resolution 3-dimensional S-wave velocity structure models for ground motion evaluation based on a joint inversion method (Sugimoto et al., 2013 [2]) integrating various kinds of geological and geophysical data.

In this paper, we report on these investigations and evaluation results.

## 2. Construction of 3-dimensional S-wave velocity structure model by joint inversion

### 2.1. Data for model construction

We carried out borehole drilling with a depth of 3,000 m at the Niigata Institute of Technology campus in 2011, and conducted strong ground motion observation by a vertical seismic array set in a borehole for about one and a half years since 2012. In addition to deep borehole observation, seismic observation by a horizontal dense array with 28 observation stations, and various kind of geophysical surveys at the surface such as microtremor array survey of 12 arrays, seismic reflection and refraction survey and gravity survey were carried out in and around this area (test site). Further, long-term microtremor array observation of 13 arrays and electromagnetic survey were conducted in the surrounding wide area.

Fig.1 (a) and (b) show the test site location and distribution of the observation stations acquired for high-resolution 3-dimensional S-wave velocity model construction. In this study, a joint inversion method was applied for model construction using the abovementioned data set, several other existing borehole data and seismic reflection profiles. The grid points to describe a global 3-dimensional model have been arranged on the microtremor array sites, seismic survey line, seismic observation stations and borehole points. Finally, 839 points of grids shown in Fig.1 (a) were used for model construction.

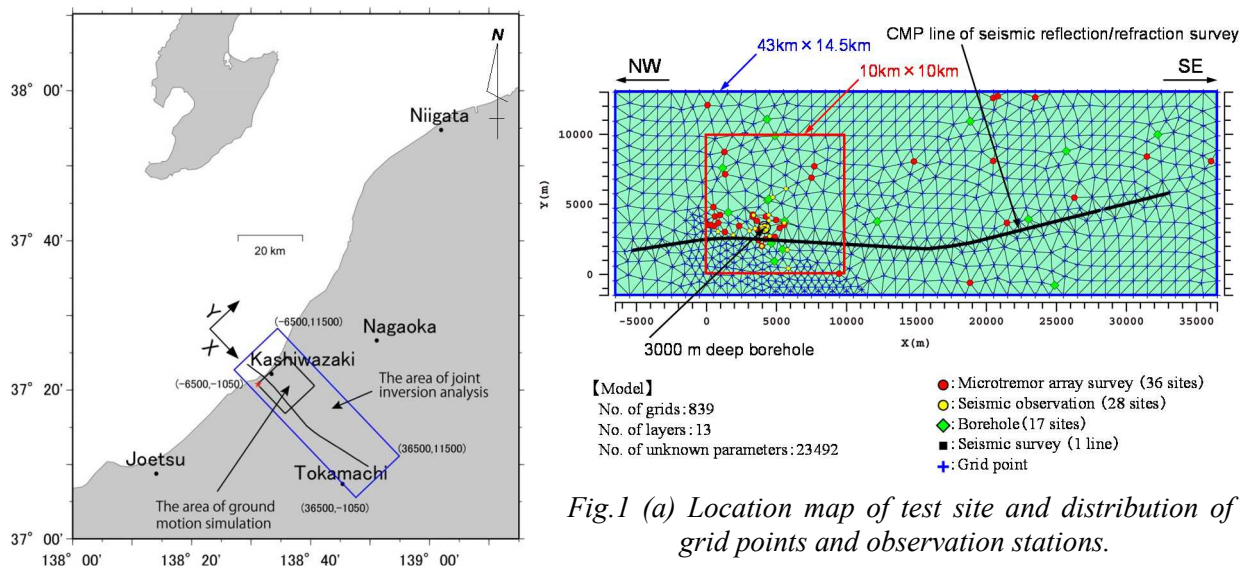


Fig.1 (a) Location map of test site and distribution of grid points and observation stations.



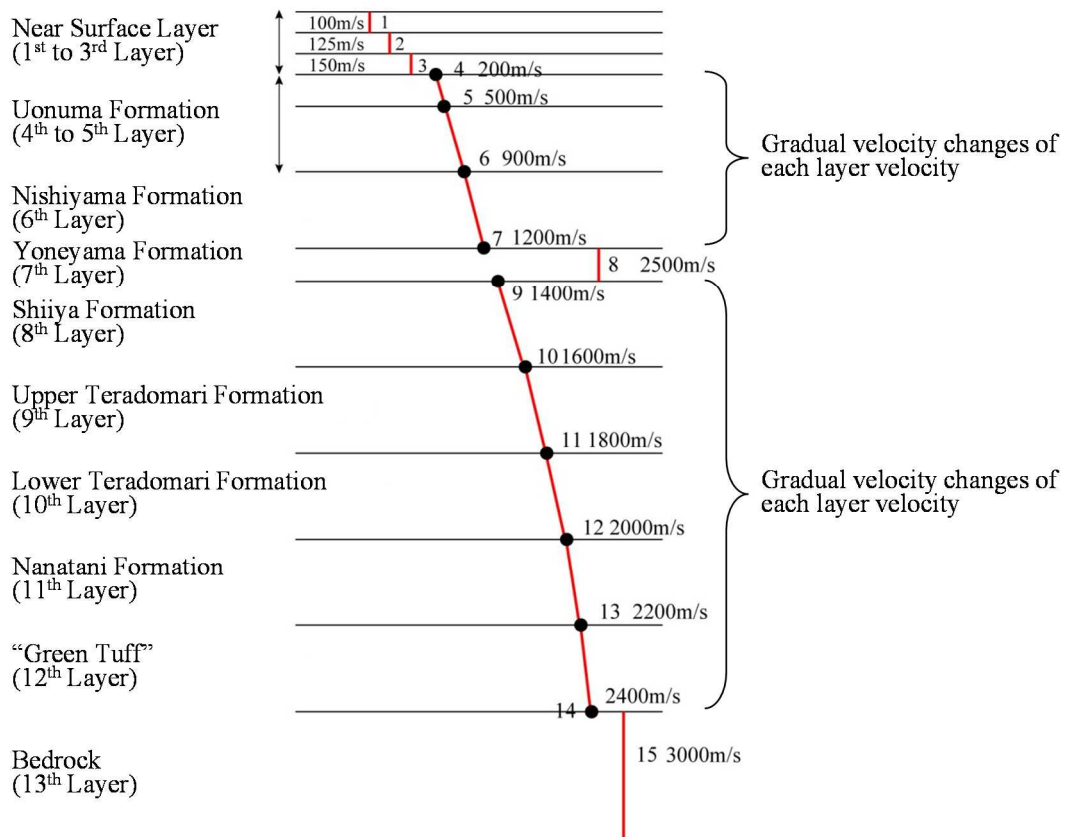


Fig.2 Initial model (1-dimensional layered model) structure at each grid point.

## 2.2. Joint inversion

In this study, we constructed two high-resolution 3-dimensional S-wave velocity structure models, called the “JNES2013A model” and “JNES2013B model,” based on a joint inversion method integrating various kinds of geological and geophysical data. The “JNES2013A model” has an inhomogeneous velocity structure in the horizontal direction within each S wave velocity layer, while the “JNES2013B model” has a constant (homogeneous) velocity structure in the horizontal direction within each S wave velocity layer.

Fig.3 shows an analysis flow of the joint inversion method. In analyzing the “JNES2013A model,” joint inversion was carried out through two steps. As the first step, the borehole, microtremor array, gravity and seismic refraction/reflection data were used for model creation. Here, the 3,000 m deep borehole data was not used for joint inversion, but was used only for verification of each 3-dimensional S-wave velocity structure model. As the second step, the SH wave spectral ratio (spectral ratio of each JNNK to JNNK 20) between two observation stations were used in addition to these survey data for model creation. For the “JNES2013B model,” joint inversion was conducted only at the first step, so we did not use the SH wave spectral ratio for analysis. RMS residuals of the “JNES2013A model” and “JNES2013B model” in the joint inversion are shown in Fig.4. To evenly reduce RMS residual of each data, the weight values for each survey data were adjusted by checking RMS residuals at several iterations. These results show that RMS residuals of both models are roughly the same.

On the other hand, in 2007, with the occurrence of the Niigata-ken Chuetsu-oki Earthquake, we constructed a conventional 3-dimensional S-wave velocity structure model, called a “JNES2007 model,” for strong ground motion evaluation. This model is based mainly on several existing borehole data and seismic reflection profiles and has a constant (homogeneous) velocity structure in the horizontal direction within each S wave velocity layer. No joint inversion was carried out in this “JNES2007 model.” In order to compare the “JNES2013A model” and “JNES2013B model” derived from the joint inversion result with the conventional “JNES2007 model,” cross sections of three S-wave velocity structure models along the seismic refraction survey line are shown in Fig.5.

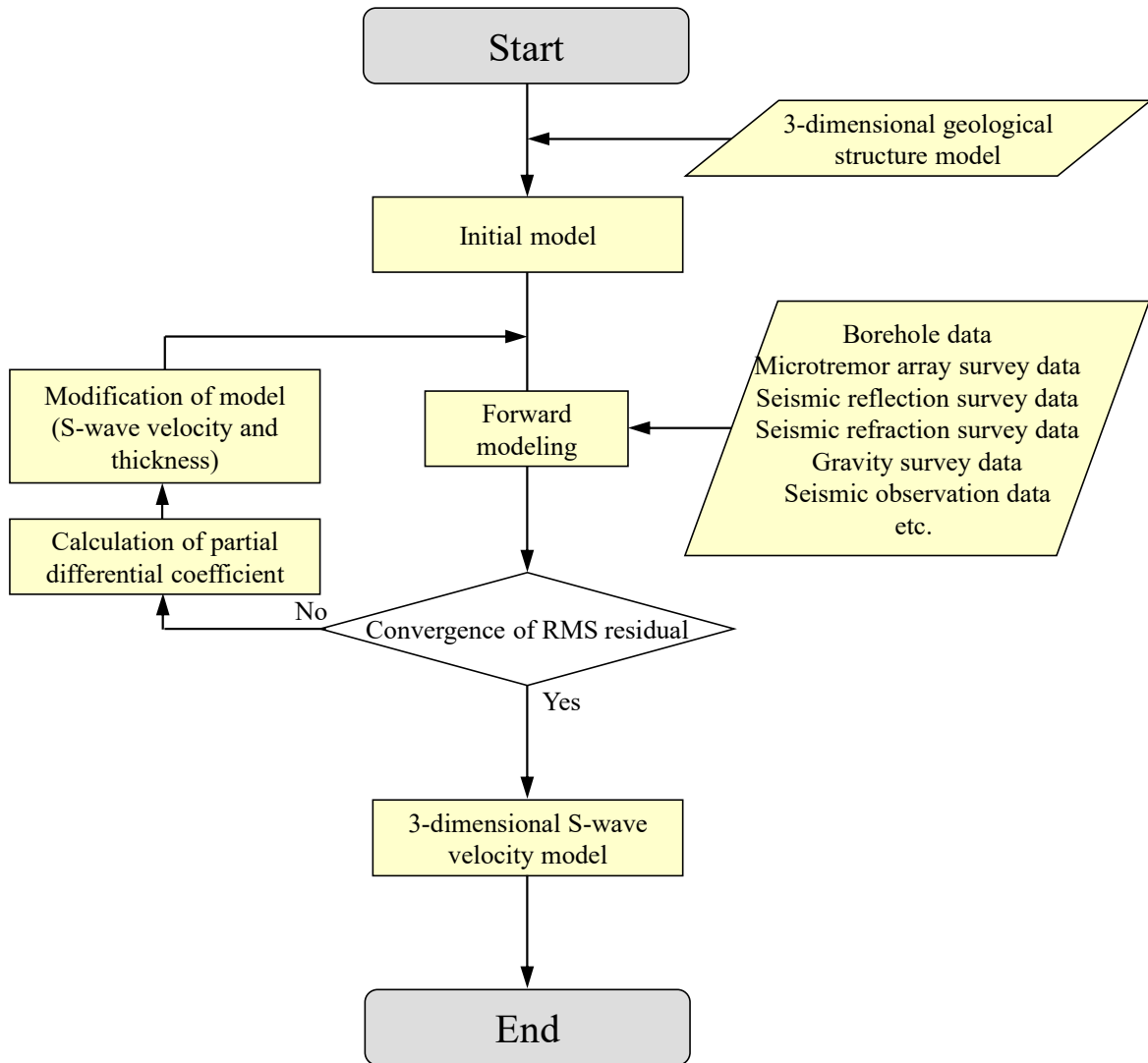


Fig.3 Analysis flow of joint inversion method.

Fig.6-9 show examples of comparison between the calculated and observed data for each geophysical survey data. These figures show that the calculated data of the “JNES2013A model” based on the joint inversion result are consistent with the observation data. On the other hand, for example, Bouguer (gravity) anomaly, the dispersion curve and SH wave spectral ratio calculated from the “JNES2007 model” shown in these figures do not sufficiently explain the observation data.

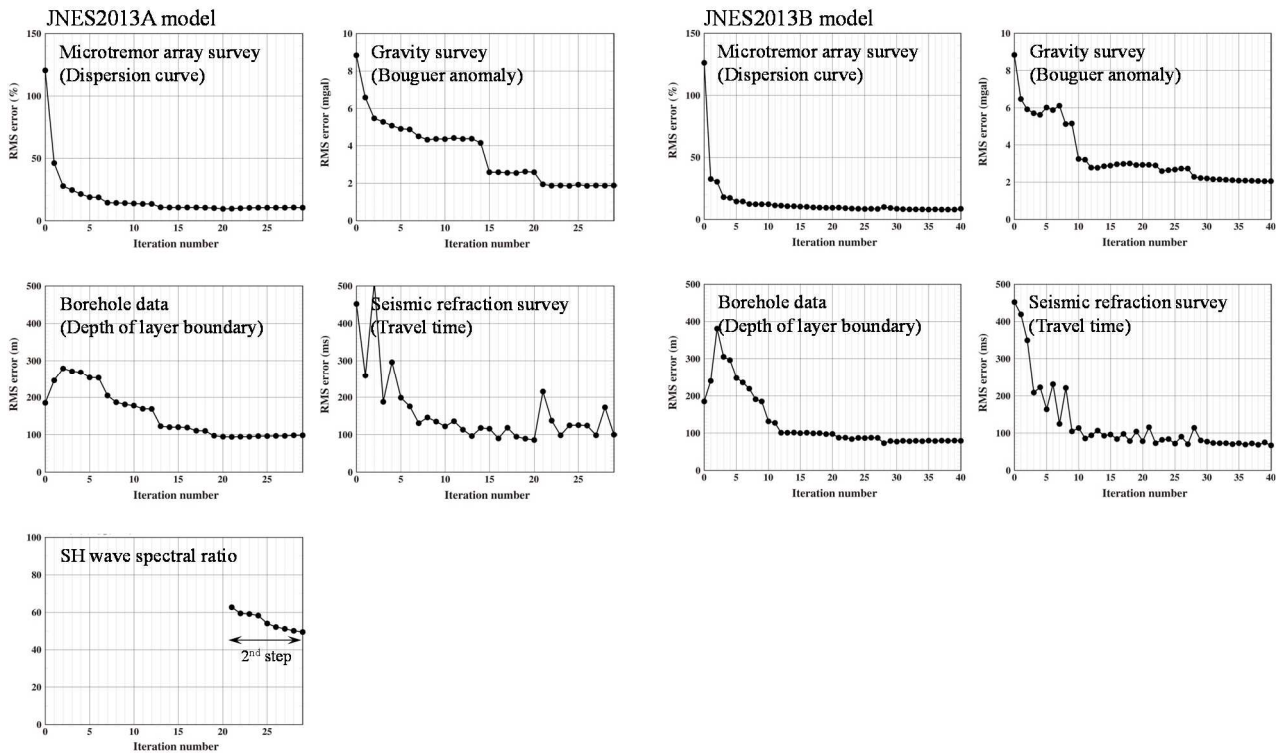


Fig.4 RMS residuals of the “JNES2013A model” and “JNES2013B model”.

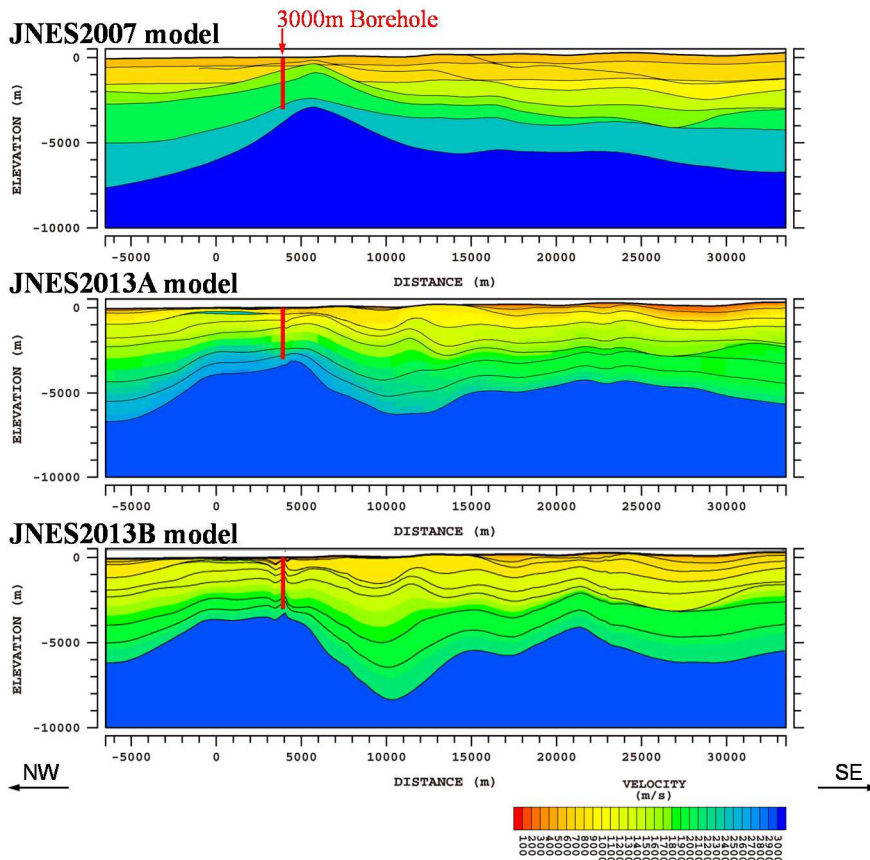


Fig.5 Cross sections of S-wave velocity structure models along seismic refraction survey line.

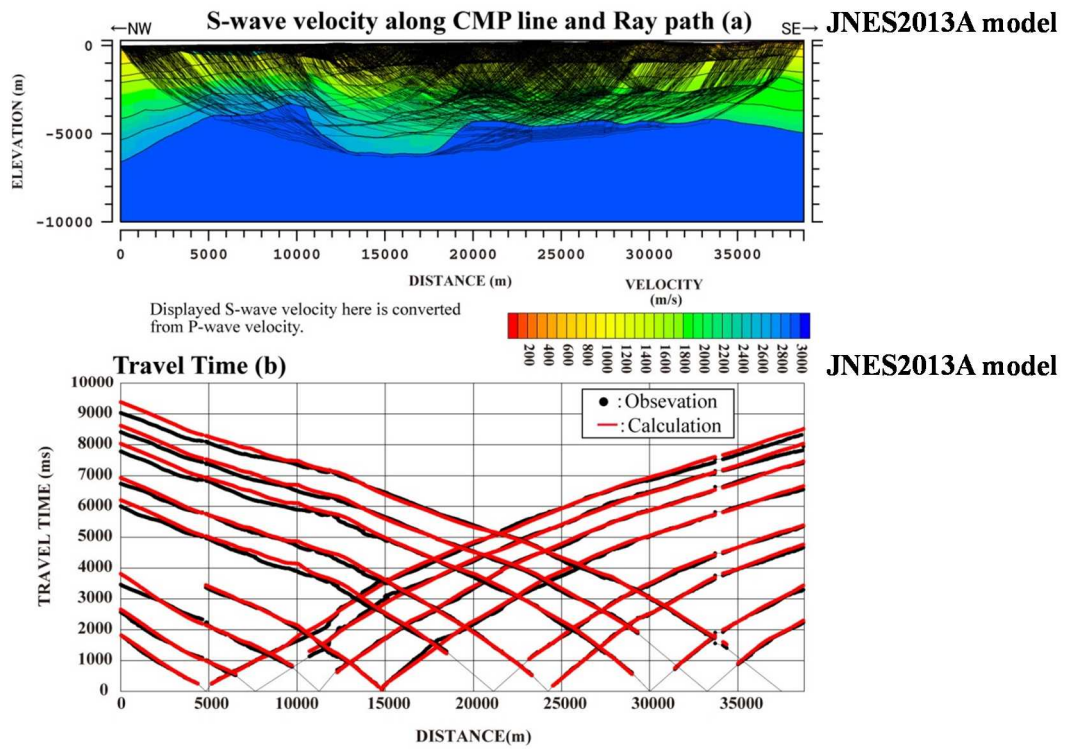


Fig.6 Comparisons between calculated and observed data for seismic refraction survey.

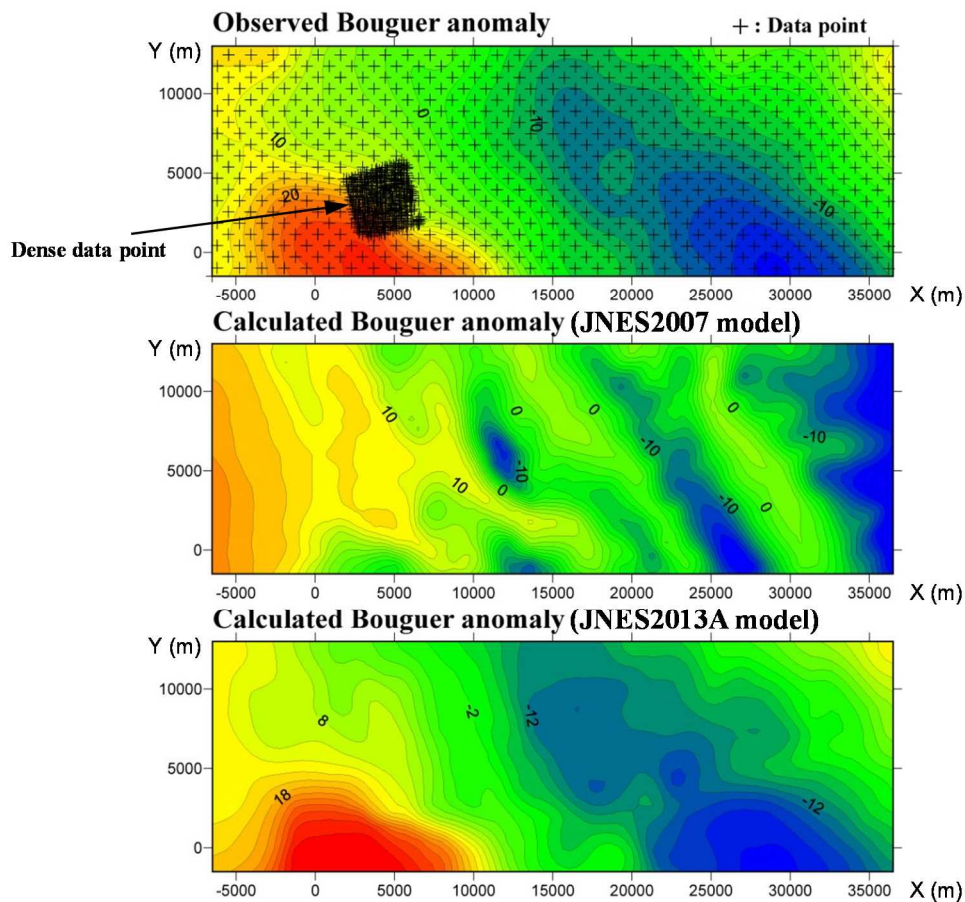


Fig.7 Comparisons between calculated and observed data for gravity survey.

Cadarache-Château, France, 14-16 May 2018

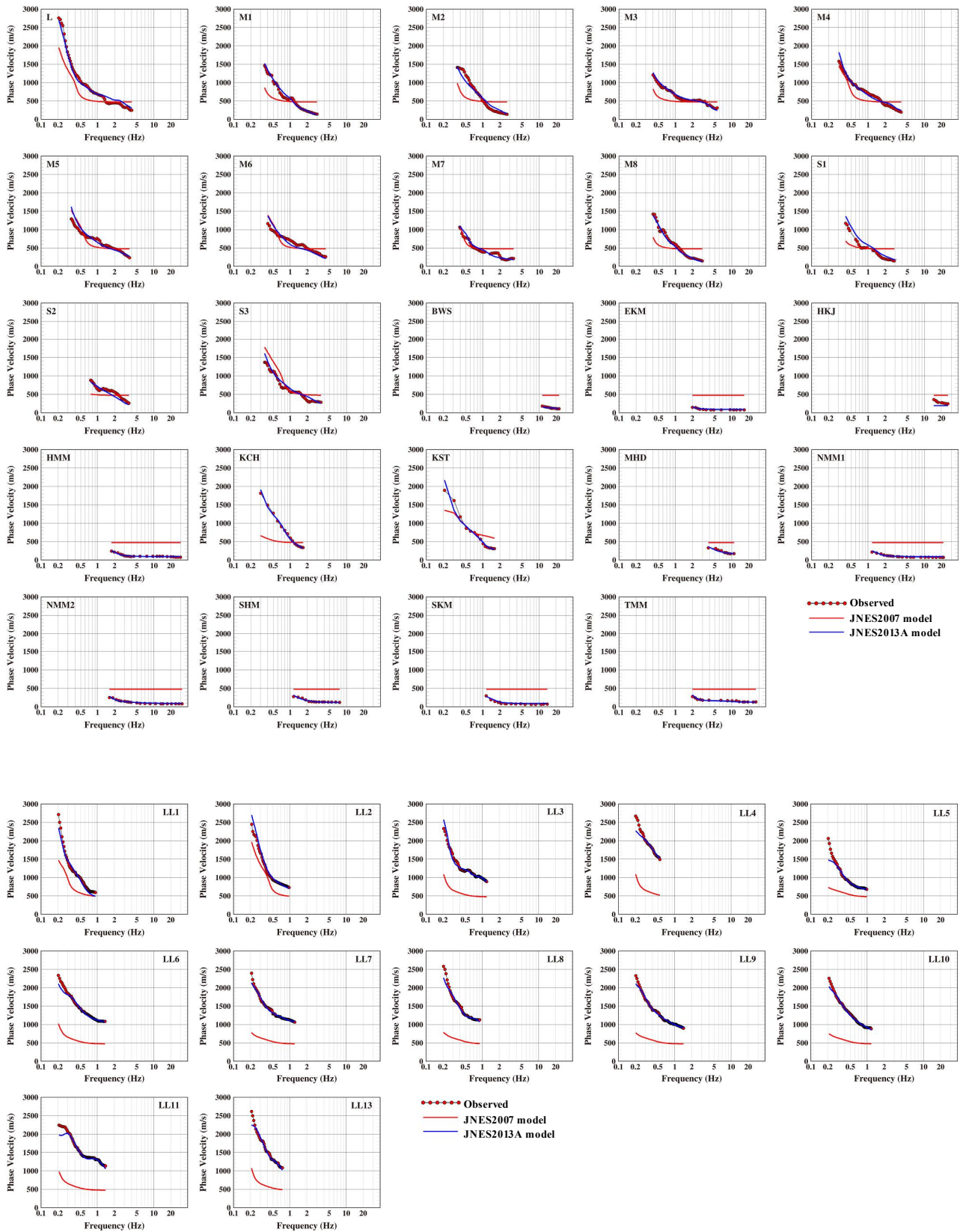


Fig.8 Comparisons between calculated and observed data for microtremor array survey.



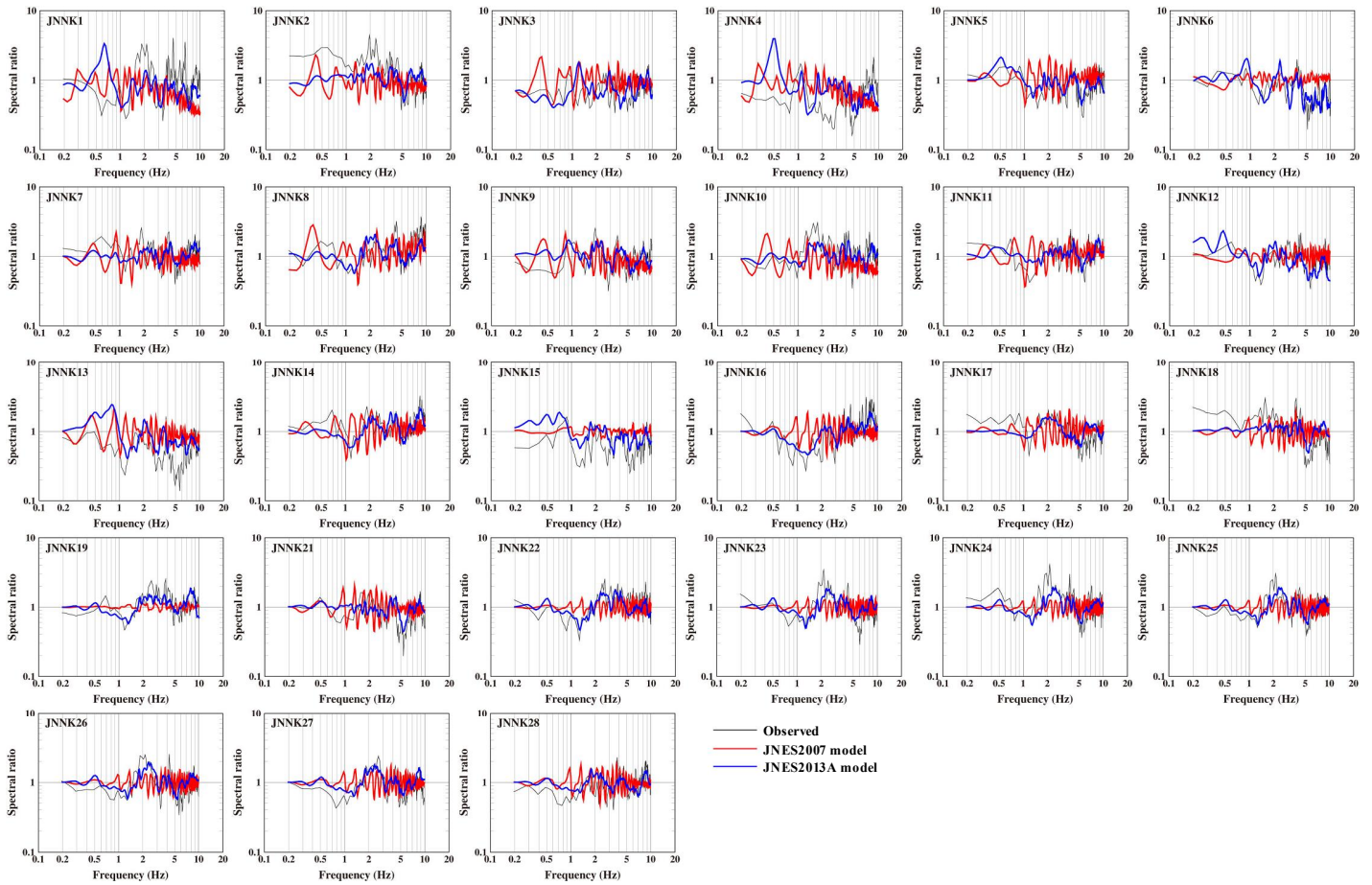


Fig.9 Comparisons between calculated and observed data for SH wave spectral ratio.

### 3. Integration of 3-dimensional S-wave velocity structure models

We carried out seismic wave propagation simulation to evaluate the accuracy of the S-wave velocity structure model using three types of 3-dimensional S-wave velocity structure models: “JNES2007 model,” “JNES2013A model” and “JNES2013B model.” First, each of the above three models was joined to the existing wide area 3-dimensional S-wave velocity structure model (hereinafter referred to as “wide area model”) constructed by the National Research Institute for Earth Science and Disaster Resilience (NIED [3]). In this study, each S-wave velocity structure model was integrated with reference to the geological structure information (Hikima, 2007 [4]).

Fig.10 shows an example of correspondence of the wide area model to three models: “JNES2007 model,” “JNES2013A model” and “JNES2013B model.” Here, we cut out the wide area model and finally created three integrated models by interpolating the “JNES2007 model,” “JNES2013A model” and “JNES2013B model,” respectively. In the rectangular range in this figure, 20 m grid data was used within the small square range and 500 m grid data was used in the outside rectangular range. Each of the strata in the three models, the “JNES2007 model,” “JNES2013A model” and “JNES2013B model,” were continuously connected with that of the wide area model.

Regarding the subsurface structures deeper than the bedrock, we used information of the deep subsurface structures of the wide area model.  $Q_s$  was set to 1/10 of S-wave velocity (m/s), and

for subsurface structures shallower than the bedrock,  $Q_s=200$  was adopted uniformly when  $Q_s > 200$ .  $Q_p$  was 1.7 times higher than  $Q_s$ .

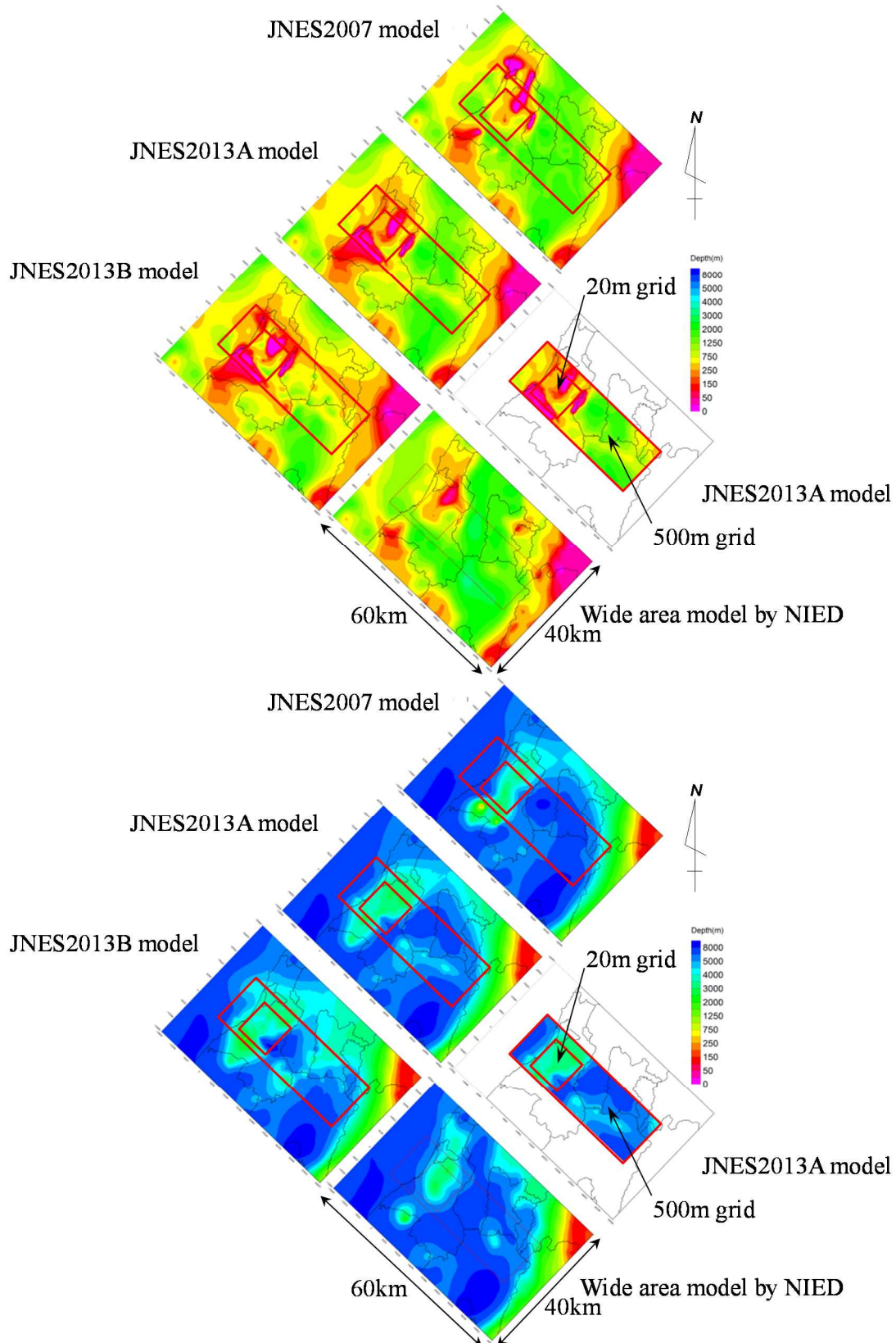


Fig.10 Example of correspondence of the wide area model (NIED) to three models: “JNES2007 model”, “JNES2013A model” and “JNES2013B model”.  
(Upper: top surface depth of Nishiyama Formation, Lower: top surface depth of bedrock)

#### 4. Seismic wave propagation simulation by 3-dimensional finite-difference method using three S-wave velocity structure models

##### 4.1. Data and model for simulation

Table 1 shows a list of the earthquakes: EQ1, EQ2 and EQ3, used in seismic wave propagation simulation, and Fig.11 shows the epicenter distribution of the earthquakes. We used the velocity–stress staggered-grid finite-difference scheme (Virieux, 1986 [5]; Levander, 1988 [6]) and used moment tensor source formulation (Graves, 1996 [7]) for modeling seismic wave propagation. In this study, since the hypocentral distance is large enough relative to the earthquake magnitude, each earthquake was assumed as a point source.

Table 2 shows specifications of the 3-dimensional finite-difference method. The minimum lattice spacing and minimum  $V_s$  of the S-wave velocity structure model were changed for each earthquake. In the calculation of the 3-dimensional finite-difference method, in the case of EQ1, it was assumed that S-wave velocity with 0.5 km/s of the engineering bedrock exists up to the ground surface. On the other hand, in the case of EQ2 and EQ3, S-wave velocity with 0.3km/s was assumed. In addition, in every case, the ground motions obtained from the 3-dimensional finite-difference method were pulled back to the engineering bedrock based on 1-dimensional multiple reflection theory. Finally, using the original (true) shallow ground model with S-wave velocity down to 0.1 km/s, the ground motions at the ground surface were recalculated from the engineering bedrock based on 1-dimensional multiple reflection theory.

Table 1 List of earthquakes used in seismic wave propagation simulation.

Event	Date	Longitude [deg.]	Latitude [deg.]	Depth [km]	Strike [deg.]	Dip [deg.]	Rake [deg.]	Mo [NM]	Rise Time [s]	Region
EQ1	2012/6/28	141.1967	37.1677	63.18	193	81	81	7.99E+16	0.5	E OFF FUKUSHIMA PREF.
EQ2	2012/10/18	138.7087	37.0277	7.07	54	55	95	2.34E+15	1.0	MID NIIGATA PREF.
EQ3	2012/7/26	138.5490	37.3595	10	32	58	94	1.10E+13	0.1	MID NIIGATA PREF.

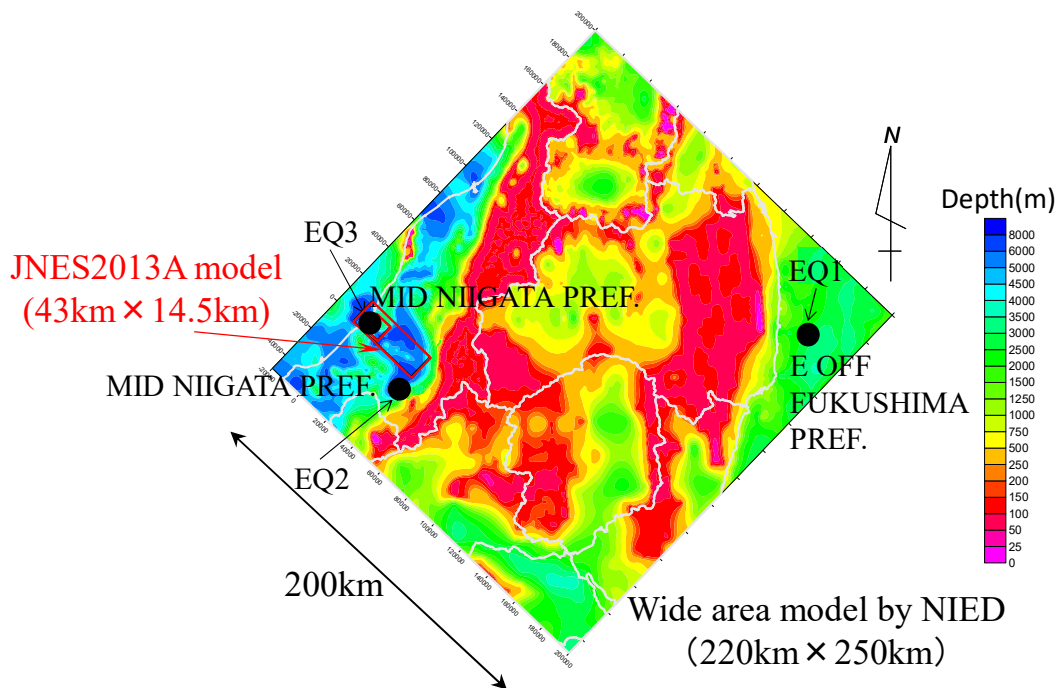


Fig.11 Epicenter distribution of earthquakes (contour plots top surface depth of bedrock).

Table 2 Specifications of 3-dimensional finite-difference method.

Earthquake	EQ1	EQ2	EQ3
Minimum grid spacing [m]	100	30	10
X-direction distance [km]	250 (Number of grid points: 2500)	75 (Number of grid points: 2500)	11 (Number of grid points: 1100)
Y-direction distance [km]	220 (Number of grid points: 2200)	45 (Number of grid points: 1500)	11 (Number of grid points: 1100)
Time increment [s]	0.01	0.003	0.001
Number of time steps	30000	30000	30000
Minimum Vs [m/s]	500	300	300
Frequency limit [Hz]	1.0	2.0	5.9

#### 4.2. Seismic wave propagation simulation results

Fig.12 (a) and (b) show simulated and observed velocity waveforms for EQ1, EQ2 and EQ3 at the 3,000 m vertical seismic array observation site. Appropriate band pass filter processing was applied to the observed waveforms in each earthquake so that they can be compared with simulated waveforms. As a result, the goodness of fit of the simulated waveform to the observed waveform decreases approximately in the order of EQ1, EQ2, and EQ3 in the “JNES2007 model” and “JNES2013B model,” and we can see the accuracy of short period ground motion is decreasing. The tendency of the decrease in the accuracy is also seen in the simulated waveforms of the horizontal seismic dense array observation.

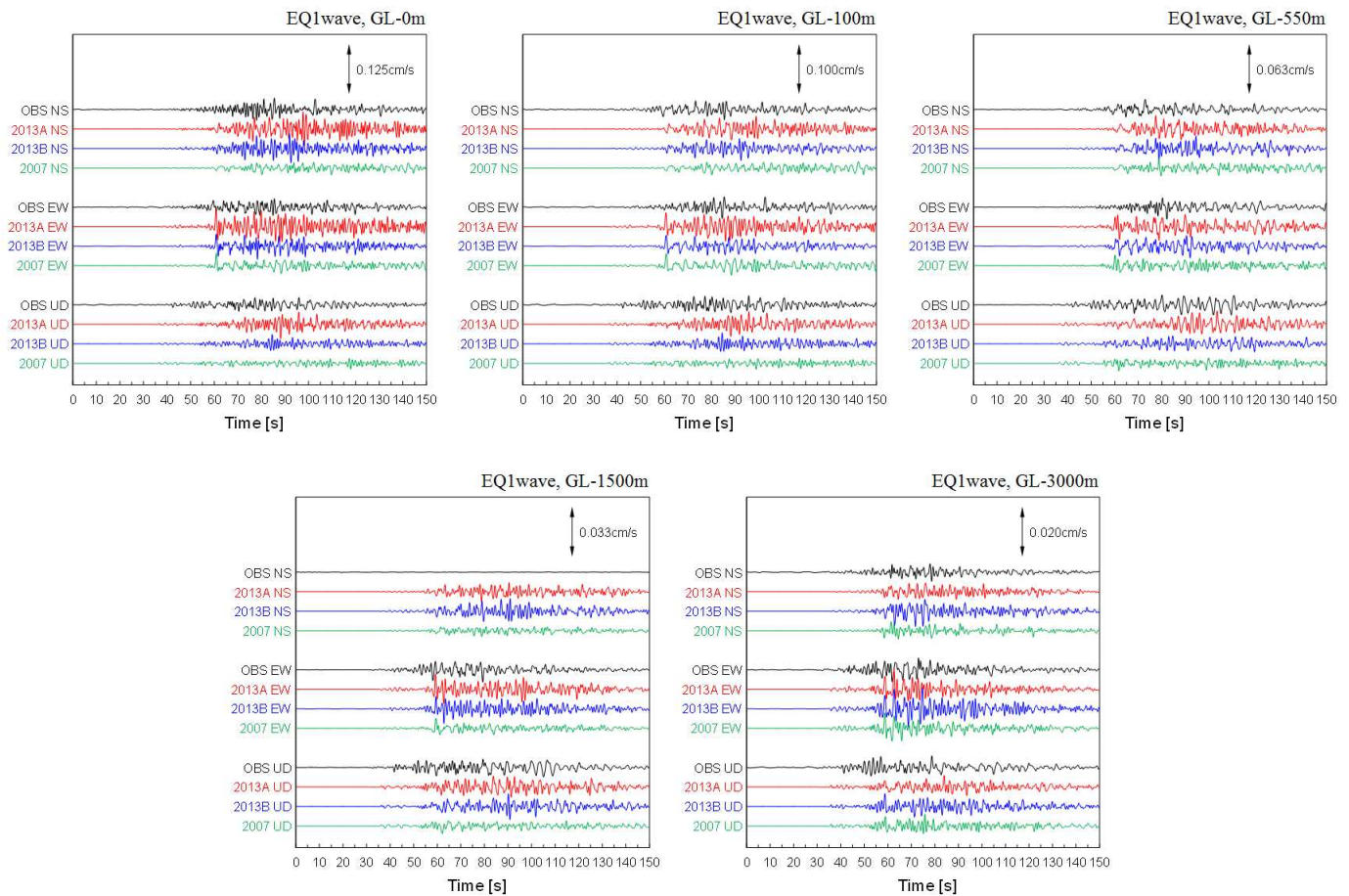


Fig.12 (a) Simulated and observed velocity waveforms for EQ1 (period of 10 to 1 s).

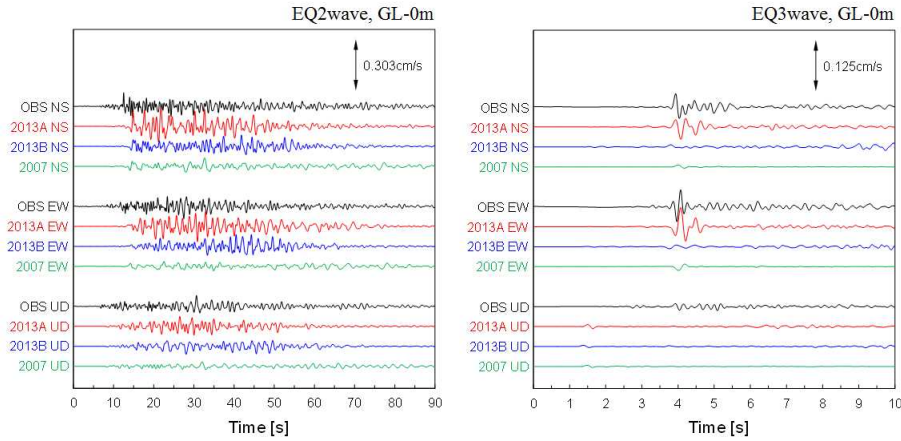


Fig.12 (b) Simulated and observed velocity waveforms for EQ2 (period of 10 to 0.5 s) and EQ3 (period of 2 to 0.2 s).

In this study, in order to evaluate the accuracy of three S-wave velocity structure models, we performed a quantitative evaluation of the simulated waveform using a score obtained by converting the Anderson score (Anderson, 2004 [8]) to 1/10. Therefore, in this study, a score below 0.4 is a “poor fit,” a score of 0.4 to 0.6 is a “fair fit,” a score of 0.6 to 0.8 is a “good fit,” and a score over 0.8 is an “excellent fit.” In the case of so-called double and half precision, the Anderson score is about 0.4. As a result, we can see that the accuracy of the S-wave velocity structure model is approximately higher in the order of the “JNES2007 model,” “JNES2013B model,” “JNES2013A model.”

Here, Fig.13 (a) and (b) show the average Anderson score of seven periodic bands (10-8 s, 8-6 s, 6-4 s, 4-2 s, 2-1 s, 1-0.5 s and 0.5-0.2 s) of three earthquakes: EQ1, EQ2, and EQ3. These figures show the average Anderson score of three earthquakes of all observation stations with respect to the velocity Fourier spectrum, pseudo velocity response spectrum and maximum velocity (PGV) of three components (NS, EW, UD), and also show the average of all three scores. As a result, the “JNES2013A model” and “JNES2013B model” show comparable good scores at a period of 2 s or longer, and furthermore, the “JNES2013A model” has a high score at a period of 1 s or less. This is because the “JNES2013B model” has a constant (homogeneous) velocity structure in the horizontal direction within each S wave velocity layer. In order to explain the ground motion in the shorter period band, it is necessary to consider the inhomogeneity in the horizontal S wave velocity layer as in the “JNES2013A model.”

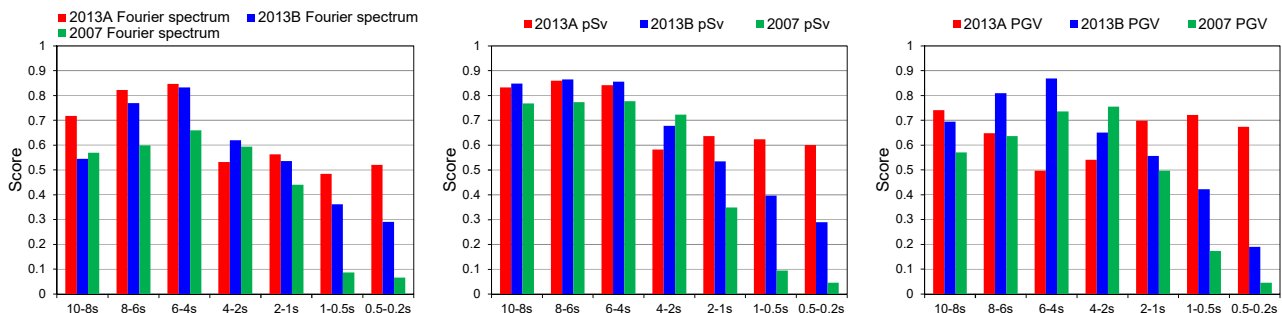


Fig.13 (a) Average Anderson score of seven periodic bands (10-8 s, 8-6 s, 6-4 s, 4-2 s, 2-1 s, 1-0.5 s and 0.5-0.2 s) of three earthquakes. (Left: velocity Fourier spectrum, Center: pseudo velocity response spectrum, Right: PGV)

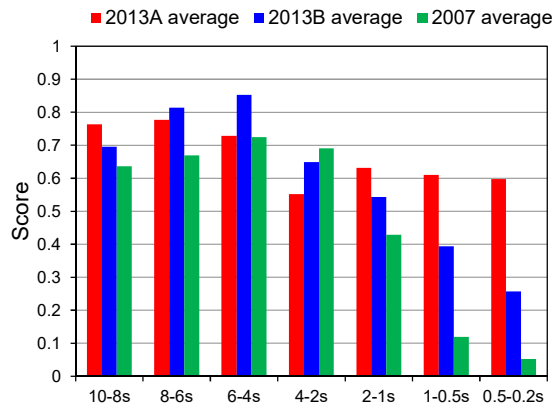


Fig.13 (b) Average Anderson score of seven periodic bands (10-8 s, 8-6 s, 6-4 s, 4-2 s, 2-1 s, 1-0.5 s and 0.5-0.2 s) of three earthquakes.

The “JNES2007 model” also shows roughly 0.6 or more at periods longer than 2 s, which is approximately a good score, but the score is extremely low at less than 1 s. This is because the “JNES2007 model” does not model the surface layer with S wave velocity of less than 0.5 km/s, which is considered to be a model with low explanation.

### 5. Evaluation of the influence of uncertainty of 3-dimensional S-wave velocity structure model on the ground motion estimation

In this study, we investigated the influence of uncertainty of 3-dimensional S-wave velocity structure model on the ground motion estimation. Fig.14 (a) and (b) show the Anderson score of each observation station for each of three earthquakes EQ1, EQ2, and EQ3 in the “JNES2013A model,” “JNES2013B model” and “JNES2007 model.” At the observation station where the Anderson score is low, there is a tendency that the score is generally lower for every earthquake, and the score tends to be generally higher at the observation station where the score is high (Fig.14 (a) and (b)).

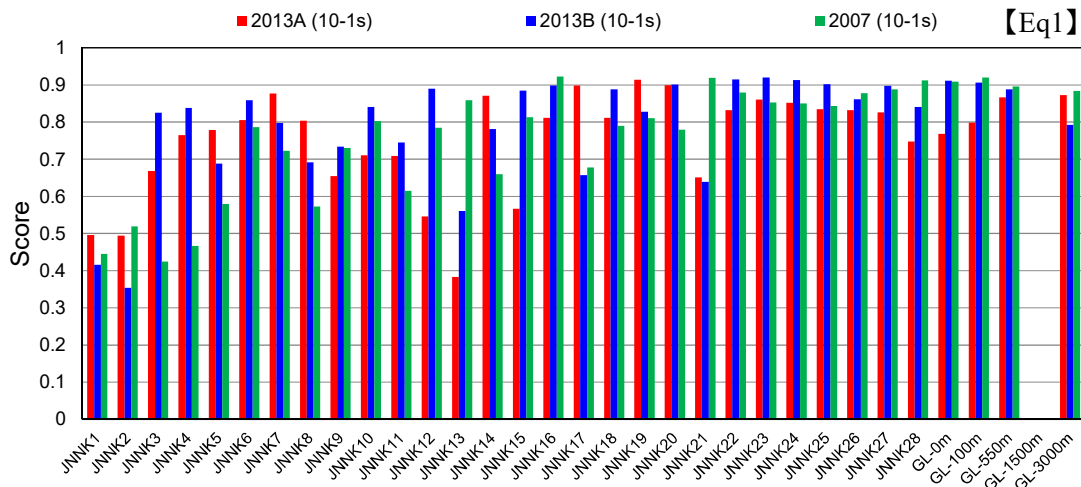


Fig.14 (a) Anderson score of each observation station for EQ1.

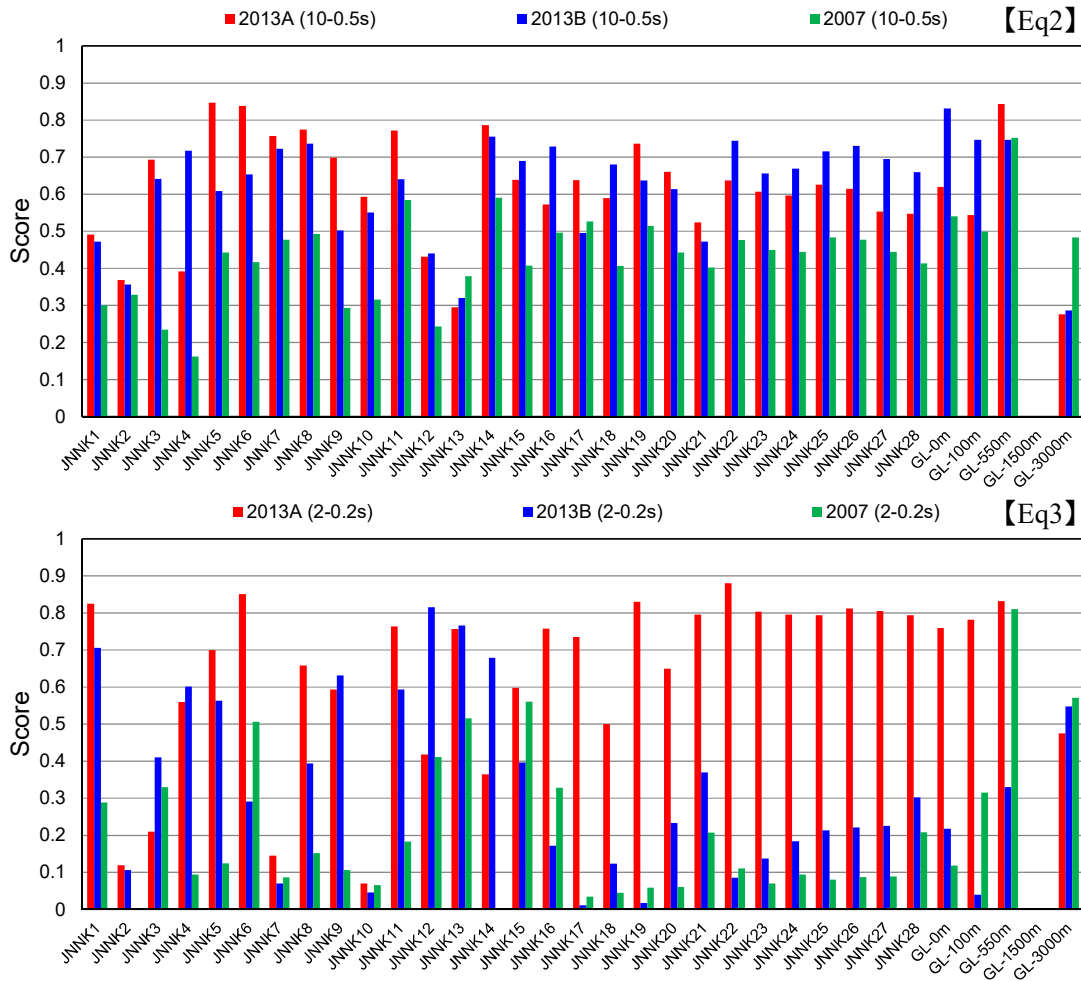


Fig.14 (b) Anderson score of each observation station for EQ2 and EQ3.

Fig.15 shows correlation of the average Anderson scores at each observation station of two earthquakes EQ1 and EQ2 in the “JNES2013A model.” EQ1 and EQ2 have a roughly positive correlation, the observation station with a high Anderson score in one earthquake has a high score even in the other earthquakes, and the low observation station has a low score in other earthquakes. This indicates that the ground motion evaluation is strongly influenced by the accuracy of the subsurface structure directly under or around the observation station. We recognize that observation stations with low Anderson scores correspond to the stations where geophysical explorations are not fully conducted. The influence of the uncertainty of the subsurface structure model on the prediction of the ground motion needs to be further investigated in the future.

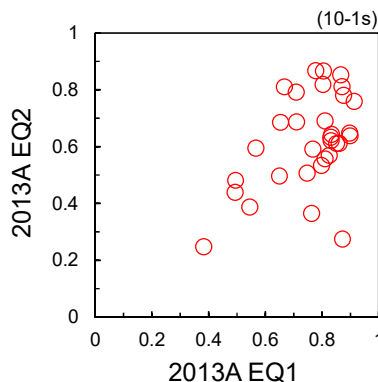


Fig.15 Correlation of the average Anderson scores at each observation station of two earthquakes EQ1 and EQ2.



## 6. CONCLUSIONS

With the occurrence of the Niigata-ken Chuetsu-oki Earthquake, we conducted a 3,000 m class deep boring that reaches bedrock equivalent to seismic bedrock as well as vertical seismic array observation at five depths of 0, 100, 550, 1,500 and 3,000 m in a deep borehole beneath the Niigata Institute of Technology campus. In addition, we conducted horizontal seismic dense array observation composed of 28 stations, and comprehensive deep subsurface structure surveys through various geophysical explorations in and around the campus.

To increase the accuracy of strong motion evaluation, we constructed high-resolution 3-dimensional S-wave velocity structure models for ground motion evaluation based on a joint inversion method, and carried out seismic wave propagation simulation. The joint inversion method makes it possible to construct a high-resolution 3-dimensional S-wave velocity structure model that can consistently explain various kinds of geological and geophysical data. In this study, we showed the accuracy of seismic wave propagation simulation of short period ground motions of 0.5-0.2 s can be improved by using a high-resolution 3-dimensional S-wave velocity structure model. We can see that the ground motion evaluation is strongly influenced by the accuracy of the subsurface structure directly under or around the observation station. The observation stations with low Anderson scores correspond to the stations where geophysical explorations are not fully conducted. In order to sufficiently explain ground motions in the shorter period band, it is necessary to consider the inhomogeneity in the horizontal direction within each S wave velocity layer of the model.

By using the model acquired by the joint inversion method, more improvement is also expected for the accuracy of the strong motion evaluation. At this stage, we have assumed that our model does not include discontinuities such as faults. A model construction with fault structures is a further challenge. We need to further investigate the influence of the uncertainty of the subsurface structure model on the prediction of the ground motion in the future.





---

## REFERENCES

- [1] JAPAN NUCLEAR ENERGY SAFETY ORGANIZATION (JNES), Guidance for construction of three-dimensional underground structure model for evaluation of earthquake ground motions, JNES-RE-Report Series, JNES-RE-2013-2016, Japan (2013) (in Japanese).
- [2] SUGIMOTO, Y., et al., Construction of 3-D S-wave velocity model by joint inversion method, Proceedings of the 11th SEGJ International Symposium, Japan (2013).
- [3] NATIONAL RESEARCH INSTITUTE FOR EARTH SCIENCE AND DISASTER RESILIENCE (NIED), [http://www.jishin.go.jp/main/chousa/12\\_choshuki/dat/](http://www.jishin.go.jp/main/chousa/12_choshuki/dat/)
- [4] HIKIMA. K., et al., Construction of 3-D velocity structure model around Niigata district, Programme and Abstracts, the Seismological Society of Japan, Fall Meeting, Japan (2007) (in Japanese).
- [5] VIRIEUX, J., P-SV wave propagation in homogeneous media: Velocity-stress difference method, Geophysics, 51, 889-901, (1986).
- [6] LEVANDER, A. R., Fourth-order finite-difference P-SV seismograms, Geophysics, 53, 1425-1436, (1988).
- [7] GRAVES, R. W., Simulating seismic wave propagation in 3D elastic media using staged-grid finite differences, Bull. Seism. Soc. Am., 86, 1091-1106, (1996).
- [8] ANDERSON, J. G., Quantitative measure of the goodness-of-fit of synthetic seismograms, 13th World Conference on Earthquake Engineering, 243, (2004).